IJE TRANSACTIONS B: Applications Vol. 39, No. 08, (August 2026) 1855-1864

International Journal of Engineering

Journal Homepage: www.ije.ir

Effects of Surface-level Defects on Tensile and Fatigue Strength of Spot Weld Bonding – Three-sheet Steel

K. Reza Kashyzadeh*[a], M. A. Ganjabi[b], S. Moghbeli[c], A. N. Ramzi Hassan[d], S. V. Khlopkov[a], M. Laad[e]

[a] *Department of Transport Equipment and Technology, Academy of Engineering, RUDN University, 6 Miklukho-Maklaya Street, Moscow, Russian Federation*
[b] *School of Mechanical Engineering, Sharif University of Technology, Tehran, Iran*
[c] *Faculty of Mechanical and Energy Engineering, Abbaspour College of Technology (ACT), Shahid Beheshti University (SBU). Tehran, Iran*
[d] *Institute of Innovation Engineering Technology, RUDN University, 6 Miklukho-Maklaya Street, Moscow, Russian Federation*
[e] *Department of Applied Sciences, Symbiosis Institute of Technology, Symbiosis International University, Pune, India*

P A P E R I N F O

Paper history:
Received 25 May 2025
Received in revised form18 September
Accepted 25 September 2025

Keywords:
Resistance Spot Welding Joint of Multiple Sheets
Resistance Spot Welding Defects
Edge Defect
Intersection Defect
Static Strength
Fatigue Behavior

A B S T R A C T

The Resistance Spot Welding (RSW) technique is a prevalent method for joining thin metal sheets, particularly in transportation-related industries such as automotive and aerospace. A key advantage of RSW lies in its efficiency and the absence of additional materials, which contribute to structural weight reduction. In this study, the influence of visible defects (i.e., edge and intersection) on the mechanical behavior of triple-layer welded joints under static and fatigue loads is analyzed. To this end, a combination of laboratory testing and Finite Element Modeling (FEM) was utilized. The FEM approach was validated using experimental axial fatigue data (high-cycle S-N curves). Unlike prior research, this investigation incorporates such as surface-level defects into the FEM framework for the first time. Simulation results showed that a 0.2 mm edge defect leads to tensile and fatigue strength decrease of 5.4 % and 13.72 %, respectively, while a 0.6 mm intersection defect for the static and fatigue strengths causes reduction of 9.6 % and 54 %, respectively. These findings highlight the fatigue strength's higher sensitivity to such defects compared to tensile strength.

***doi**: 10.5829/ije.2026.39.08b.07*

Graphical Abstract

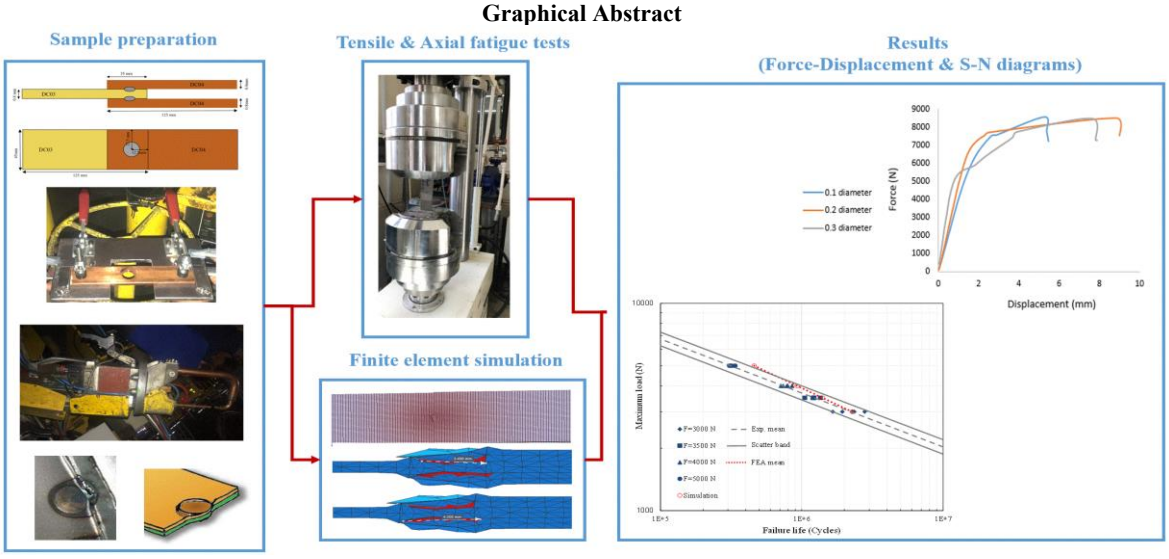

*Corresponding Author Email: reza-kashi-zade-ka@rudn.ru (K. Reza Kashyzadeh)

Please cite this article as: Reza Kashyzadeh K, Ganjabi MA, Moghbeli S, Ramzi Hassan AN, Khlopkov SV, Laad M. Effects of Surface-level Defects on Tensile and Fatigue Strength of Spot Weld Bonding – Three-sheet Steel. International Journal of Engineering, Transactions B: Applications. 2026;39(08):1855-64.

1. INTRODUCTION

Various resistance welding methods, such as RSW, Resistance Seam Welding (RSEW), and Projection Welding (PW), are implemented across transportation sectors including automotive, shipbuilding, aerospace, and helicopter manufacturing (1, 2). Among these, RSW is especially popular due to its efficiency, minimal cost, and industrial suitability (3). RSW operates by heating metal sheets to a plastic state using an electric current and applying pressure to form a compact weld zone known as the nugget (4). Despite its advantages, RSW is prone to manufacturing defects, which compromise joint durability (5). Focusing on defects and solutions is beyond the scope of this paper. The focus here is on evaluating how defects affect joint strength. Undersized welds, characterized by a nugget diameter smaller than the optimal threshold (denoted by "IM"), are a common defect type that significantly compromises joint performance under various loading conditions (6). RSW defects can be detected using both Destructive Testing (DT) and Non-Destructive Testing (NDT) methods, such as ultrasonic inspection. Today, a combination of different methods is used to defect detection. For example, Liu et al. (7) presented a novel faster R-CNN model to detect RSW defects through visual inspection. They reported that they could process each image at a speed of 15 milliseconds using this model. The accuracy of the presented model was also stated to be more than 90%. However, in industrial settings, DT is primarily used to validate the accuracy of NDT interpretations, as DT renders the component unusable. Hence, the identification, characterization, and dimensional assessment of weld defects is critical to understanding their impact on structural performance under operational conditions.

Summerville et al. (8) introduced an advanced technique for estimating nugget diameter using dynamic resistance curves combined with Principal Component Analysis (PCA), Auto-Correction (AC), and Multi-Linear Regression (MLR), which outperformed conventional C-scan methods in accuracy. Mirzaei et al. (9) highlighted the dominant influence of welding current on nugget formation in galvanized steel sheets and observed a positive correlation between nugget size and joint strength up to a limit, beyond which performance declined (10). Moreover, Eisazadeh et al. (11) reported in their study that various parameters affect the nugget diameter, but among them, the highest percentage by weight belongs to the electric current. However, accurate RSW assessment remains challenging and results in additional costs and production steps. Current inspection methods, which rely on random inspections after vehicles leave the body-in-white (BIW), often result in significant time wastage and emphasize the need for improved quality assessment. To overcome this issue, researchers have turned to data analytics approaches as well as machine learning techniques to predict the weld quality level before the vehicle body is completed. Recently, the performance of various algorithms including Artificial Neural Network (ANN), Convolutional Neural Network (CNN), Long Short-Term Memory (LSTM), Random Forest Classifier (RFC), and Extreme Gradient Boosting (XGBoost) has been investigated and it is shown that with the help of such algorithms, the accuracy of RSW defect prediction can be increased to 97.1% (12).

A new FEM based on Mechanical-Electrical-Thermal (MET) coupling has been used to investigate the weld core diameter and consequently the weld strength of two-sheet 304 steel (13). Farrahi et al. (14) utilized various numerical methods to predict the fatigue life of automotive spot welds, revealing that although modal dynamic analysis is significantly more time-consuming than the inertial relief approach, both yield comparable accuracy under low-frequency loading. Pan and Sheppard (15) employed FEM to predict fatigue behavior in spot welds of sheets with varying thicknesses, while Reza Kashyzadeh and Ghorbani (16) proposed an empirical model relating High-Cycle Fatigue (HCF) performance to chemical composition in three-sheet, low-carbon spot welds. Deshmukh and Kharche (17) used the response surface methodology to optimize the spot welding process parameters including pressure time, welding time, holding time, and electrode force to improve the joint quality of 316L sheets and ultimately their strength under static and cyclic loading. They reported that the most optimal case included 33, 12, and 9 cycles for pressure, welding, and holding times, respectively. Also, the electrode pressure was proposed to be 2.8 bar.

Residual stress distribution in RSW joints has also been modeled using FEM and validated against X-ray diffraction data (18). Findings indicate that peak residual stress occurs at the weld center and decreases toward the periphery. Numerous studies affirm that residual stress distribution, including its location and magnitude, is a key parameter in fatigue life estimation (19, 20). Pal and Bhowmick (21) compared DT (tensile testing) and NDT (peel testing) on DP780 steel sheets, concluding that tensile testing yields superior precision. They also reported that modifying current and time parameters significantly affects Low-Cycle Fatigue (LCF) behavior. Xiao et al. (22) found that refined microstructures in the fusion zone improve fatigue resistance compared to coarser structures due to twin formation and multiple pyramidal slips, which help reduce stress concentration.

Ordoñez et al. (23) investigated stress concentration effects on crack initiation in DP980 steel, finding that the number, arrangement, and spacing of sopt welds are critical factors affecting fatigue life (24, 25). Vural et al. (26) examined how nugget diameter impacts fatigue performance in dissimilar joints of AISI 304 stainless steel and galvanized steel. Recent work by Farrahi et al. (6) combined finite element and multi-body dynamic

simulations to evaluate the impact of vehicle speed and road surface irregularities on weld failure across vehicle structures. They observed that variations in nugget diameter could alter fatigue life by up to 100%. Furthermore, their latest research explored the effects of electrode geometry on residual stress distribution and subsequent fatigue performance in three-sheet joints (27). Previous research has extensively focused on fatigue behavior in defect-free welds or welds with insufficient nugget formation. In addition, with the aim of enhancing fatigue behavior, many efforts have been made to optimize RSW process parameters through traditional, classical, and modern techniques (28). The present study uniquely investigates the impact of visible surface defects, a category traditionally considered non-critical, on fatigue performance. Based on industrial experience, the authors argue that such defects, edge and intersection, should be reclassified as quasi-strength defects due to their measurable influence on joint strength. This hypothesus is explored through a collaborative effort between academia and a major automotive manufacturer. Therefore, the primary purpose of this study is to quantitatively evaluate the effects of edge and intersection defects on the static tensile strength and high-cycle fatigue behavior of three-sheet steel spot weld bonding joints. To achieve this, a combined experimental and numerical approach was employed. Firstly, experimental S-N curves for healthy joints were established to serve as a validation benchmark. Subsequently, an advanced finite element model, incorporating Electrical-Thermal-Mechanical coupling and metallurgical phase transformation, was developed and validated. This validated model was then used to systematically simulate the mechanical response of joints with varying severities of edge and intersection defects under both static and cyclic loading conditions. Ultimately, this work aims to provide robust data to support a re-evaluation of quality control standards for visible defects in automotive spot welding.

In the following, a schematic diagram of the spot weld categorized examined in the current study, including health spot weld and the desired apparent defects, is shown in Figure 1.

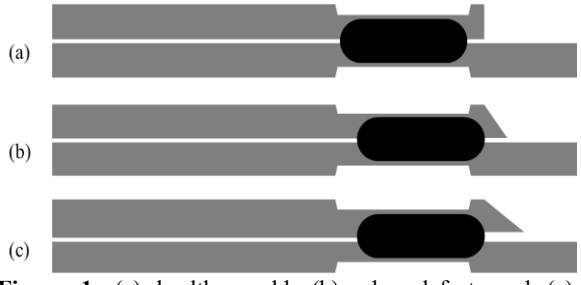

Figure 1. (a) healthy weld, (b) edge defect, and (c) intersection defect

According to the manufacturer's data (e.g., sheet material, sheet thickness, welding parameters, etc.), the nugget diameter for a healthy weld is 4 mm (Figure 1(a)). The difference between desired defects is that if the edge is between zero and 1/3 of the nugget diameter, it is called an edge defect (Figure 1(b)), and if this size is more than 1/3 of the nugget diameter, it is called intersection defect (Figure 1(c)).

2. MATERIALS AND SPECIMEN PREPARATION

According to prior investigations (3, 29) and internal data provided by the automotive manufacturer, the most structurally sensitive spot weld in a three-sheet automotive joint comprises dissimilar low-carbon steel grades. Specifically, two DC04 sheets are placed at the top and bottom of the joint and the DC03 sheet is placed between them. However, the thickness of all sheets is the same and equal to 0.8 mm. Figure 2(a) shows the sheets' dimensions and their arrangement for a healthy spot weld joint. To prepare the specimens uniformly, a fixture designed and fabricated in previous work was used (Figure 2(b)).

The engineering specifications of the sheets used in this study, DC04, and DC03, are given in Tables 1 and 2, respectively. All of this information was obtained in a laboratory setting (e.g., tensile test, metallographic examination of microstructure, and quantometric analysis) on the factory production line before being used.

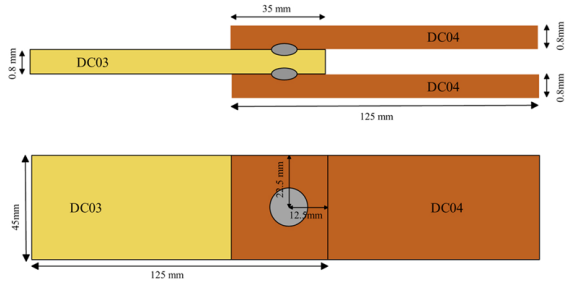

(a)

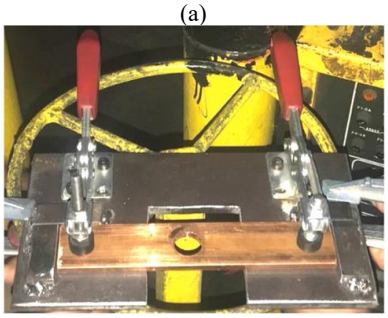

(b)

Figure 2. (a) Size and layout of three-sheet spot-welded joint in a free-defect state and (b) Fixture used to prepare a healthy connection

The welding parameters were considered to create a healthy three-sheet spot-welded joint as it is done in the automotive industry (Table 3). Also, the standard electrode F0-16-20-8, as shown in Figure 3(a), was used for this purpose (27). Figure 3(b) demonstrates the manual welding equipment used in this industry. The frequency was 50 Hz, and the electric current was alternating.

TABLE 1. Engineering specifications for DC04 low-carbon steel

Chemical composition	
Base	Fe
C	0.046 %
Si	0.014 %
Mn	0.201 %
P	0.007 %
S	0.004 %
Al	0.036 %
Mechanical properties	
Yield Strength: YS	169 MPa
Ultimate Tensile Strength: UTS	307 MPa
Elongation: E	38 %
Microstructure features	
Metallic phase	Ferrite
Average grain diameter	31.8 µm

TABLE 2. Engineering specifications for DC03 low-carbon steel

Chemical composition	
Base	Fe
C	0.047 %
Si	0.006 %
Mn	0.199 %
P	0.007 %
S	0.004 %
Al	0.037 %
Mechanical properties	
Yield Strength: YS	178 MPa
Ultimate Tensile Strength: UTS	325 MPa
Elongation: E	41 %
Microstructure features	
Metallic phase	Ferrite
Average grain diameter	30.2 µm

TABLE 3. Default factory-configured parameters for the spot welding process aimed at producing a defect-free joint (28)

Welding parameters	**Value [Unit]**
Force	365 [N]
Current	11.5 [KA]
Squeeze time	25 [Cycle]
Upslope	3 [Cycle]
Welding time	12 [Cycle]
Hold time	9 [Cycle]

3. EXPERIMENTAL PROCEDURE

As outlined earlier, a weld is considered structurally sound when the minimum nugget diameter reaches at least 4 mm. In a three-sheet spot weld configuration, two individual nuggets are formed: one between the top and middle layers and another between the middle and bottom layers. Hence, a 4 mm threshold is set as the minimum acceptable nugget diameter. Although some previous studies overlook the distinction between these two nuggets and report only their average, this investigation accounts for both individually.

Defect-free welded specimens were initially fabricated and then sectioned to enable cross-sectional analysis. The nugget diameters were measured using Optical Microscopy (OM), yielding an average size of

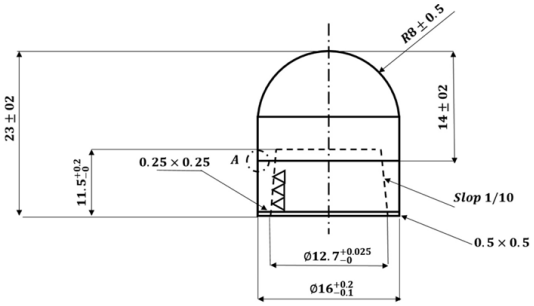

(a)

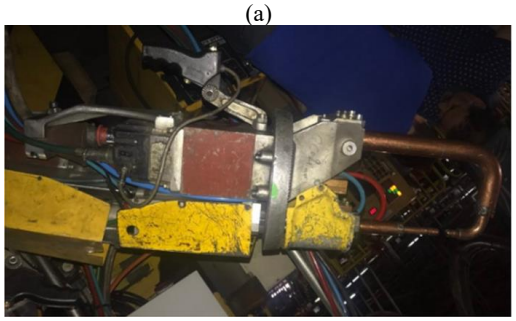

(b)

Figure 3. (a) Geometry and dimensions (mm) of F0-16-20-8 standard electrode (27) and (b) Manual welding equipment used in the current study

approximately 5.55 mm, well above the required minimum of 4mm. Consequently, the welding settings recommended by the manufacturer were adopted for the preparation of all specimens. A total of 28 healthy three-sheet spot-welded specimens were fabricated. Fatigue testing was conducted using a servo-hydraulic axial loading system with a 25-ton capacity. To maintain uniform thickness and prevent bending during testing, steel plates were added symmetrically to both sides of the specimen. This ensured a consistent grip thickness of 4 mm at the clamping region, according to ISO 14324 guidelines (30). All fatigue tests were carried out at room temperature using a force-controlled, constant amplitude protocol. The loading followed a sinusoidal waveform with a force ratio (R) near zero and a frequency of 10 Hz. Multiple loading levels were applied, and for each level, seven identical specimens were tested to account for potential scatter and improve the statistical robustness of the results. The mean number of cycles to failure from these seven specimens was taken as the representative fatigue life for that force level. Ultimately, a force-life curve in the HCF regime was established for the healthy three-sheet spot-welded configuration.

4. FINITE ELEMENT SIMULATION

To model the spot welding process with consideration of various surface-level defects, an enhanced version of the finite element algorithm (originally introduced in the authors' recent publication) was employed (29). While the initial version of the algorithm focused on simulating welds with internal strength-related defects such as IM (insufficient nugget), the updated model extends its capabilities to incorporate visible anomalies. Parameter inputs for the welding process were derived from industrial datasets, and the numerical simulation was executed via an integrated platform combining commercial finite element software with MATLAB scripting. This allowed for predictive modeling of nugget diameter as a function of input process parameters. A notable strength of this updated algorithm lies in its multi-physics coupling, treating the welding operation as a fully integrated Electrical-Thermal-Mechanical (ETM) system. Moreover, the algorithm accounts for material-specific metallurgical behavior, thereby increasing fidelity in predicting weld formation. The material properties used in the simulation were not generic values but rather obtained through prior experimental characterization based on raw material attributes and grain structure. To capture phase transitions during the welding cycle, both Time-Temperature-Transformation (TTT) and Continuous Cooling Transformation (CCT) diagrams were integrated into the simulation workflow. These diagrams enabled realistic modeling of the fusion zone's thermal evaluation and its effect on microstructural development.

To reduce computational costs while maintaining the accuracy of the responses, the mesh sensitivity analysis was performed considering three different element sizes including 1, 0.8, and 0.5 mm. Also, in the weld zone with a diameter of approximately 7 mm, the meshes were refined two times. In other words, the element sizes in the weld zone for the three models were 0.25, 0.2 and 0.125 mm, respectively. The results of this analysis based on the von Mises equivalent stress criterion are presented in Table 4.

All three models have a small difference up to a distance of 5 mm from the weld center, but in the two models with overall element sizes of 0.5 and 0.8 mm, the difference in results increases significantly from a distance of 5 to 7 mm. While the error rate in this range for the two models with mesh sizes of 1 mm and 0.8 mm is still an acceptable value. This shows that as the mesh sizes become smaller, the accuracy of the solution at distances of 5 to 7 mm decreases sharply. Therefore, a mesh size of 1 mm with two times refinement in the weld zone was chosen for future simulations. In this case, the number of elements in the FE model is 33,750. All the above explanations were valid for the simulation of the healthy weld. However, when the apparent defects are modeled, due to the plastic deformations created in the weld area and the asymmetric contacts of the electrode tip with the sheets, the refined elements caused the response to diverge. Therefore, in the simulations of the connection with the desired defects, only mesh size of one millimeter was used throughout the sample. Figure 4 provides a schematic representation of the full algorithm used to simulate spot welds with apparent defects.

For fatigue analysis, the Battelle structural stress methodology was adopted. This approach offers a mesh-intensitive framework and has been widely validated for fatigue life estimation across various welded steel components. Its effectiveness is based on the master S-N curve approach, particularly for different steels (31), and is described by the following equation:

TABLE 4. Mesh sensitivity analysis results for spot weld bonding – three-sheet steel

Distance from weld center (mm)	Element size (mm)		
	1	**0.8**	**0.5**
0	6	5.54	6.11
1	5.97	5.75	6.07
2	5.89	5.39	5.12
3	5.8	5.17	4.97
4	5.46	5.4	5.72
5	4.63	5.51	5.59
6	30.1	34.93	13.42
7	102.7	103.7	87.6

$$\Delta S_x = CN_f^h \quad (1)$$

Here, ΔS_x denotes the structural stress range, and N_f is the number of cycles to failure, and C and h are material-specific constants for steels. The values of these coefficients are summarized in Table 5 (32). An overview of the fatigue evaluation algorithm used in this study, from simulation to life prediction, is depicted in Figure 5.

TABLE 5. Material-specific constants for the master S-N curve applied to steels [33]

Statistical base	C (MPa)	Hold time
Mean	19930.2	
+2σ	28625.5	
−2σ	13875.8	-0.32
+3σ	31796.1	
−3σ	12492.6	

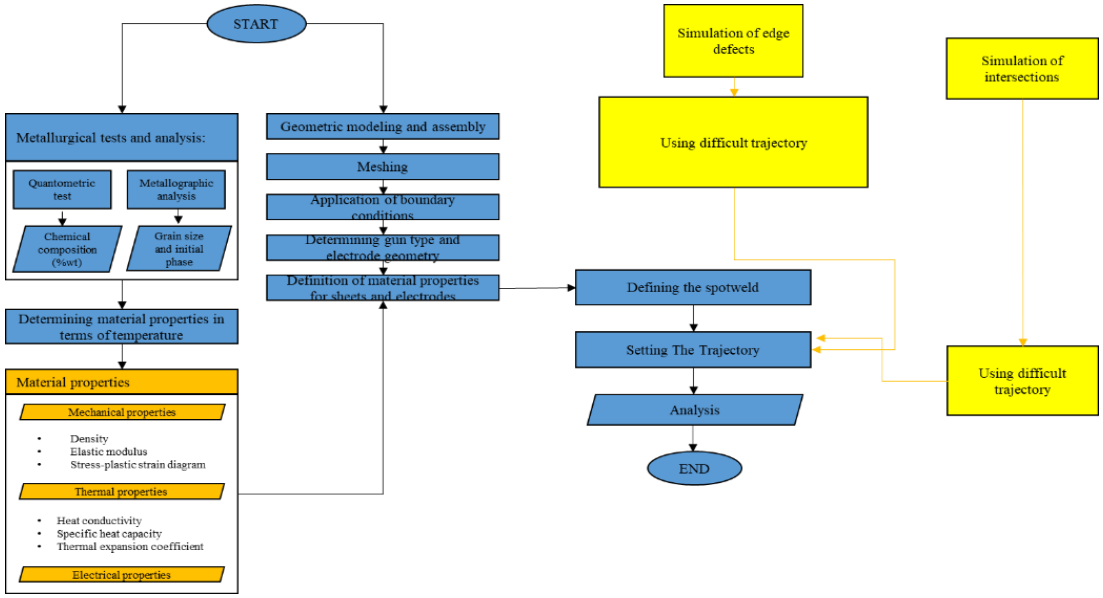

Figure 4. The framework of the updated 3D finite element algorithm is employed to simulate the spot welding process with distinct surface-level defects

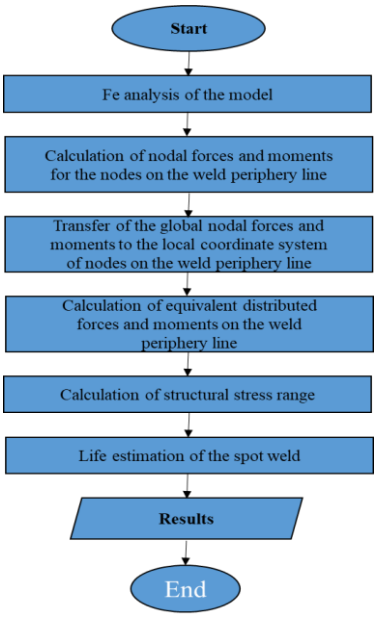

Figure 5. Workflow of fatigue life assessment of the RSW joint utilizing the Battelle structural approach [28]

4. 1. Analysis of Edge-affected RSW Joints As mentioned earlier, this defect is caused by the incorrect position of the weld core with the sheets' edges. If the size of the apparent defect is less than or equal to 0.33 of the nugget diameter, it is called an edge defect. Therefore, in this study, three different intensities for edge defect (0.1, 0.2, and 0.3 of the nugget diameter in a healthy joint) were considered. The finite element model as well as the diameter of the weld nugget after the process are illustrated in Figure 6.

4. 2. Analysis of Intersection-affected RSW Joints As previously shown, an intersection defect is described when the edge defect exceeds one-third of the nugget diameter. The characteristic of the simulation example of this defect, i.e., 0.8, is demonstrated in Figure 7.

5. RESULTS AND DISCUSSION

5. 1. Validation of Finite Element Analysis Figure 8 presents a comparison between the numerical

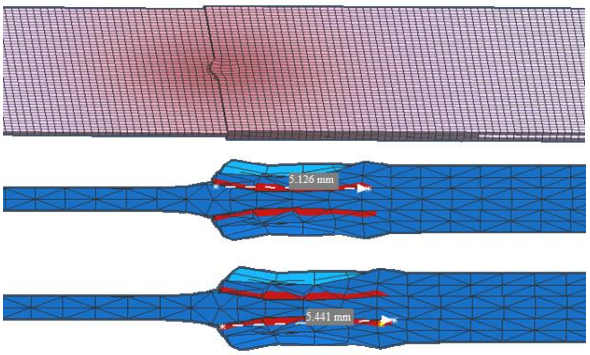

Figure 6. FEM and weld nugget diameter for three-sheet spot-welded joint with edge defect considering the intensity of 0.3 nugget diameter as a representative

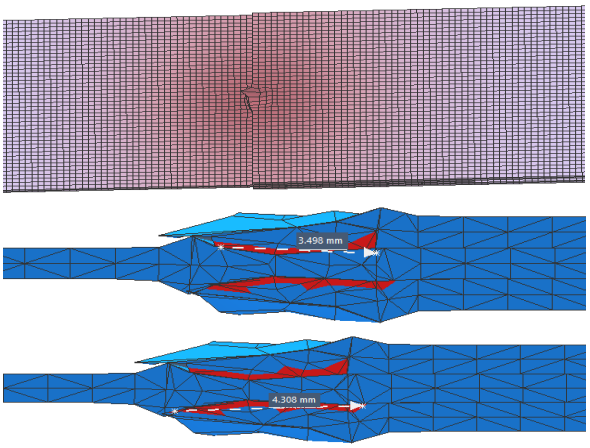

Figure 7. FEM and weld nugget diameter of RSW joint with intersection defect considering the intensity of 0.8 as a representative

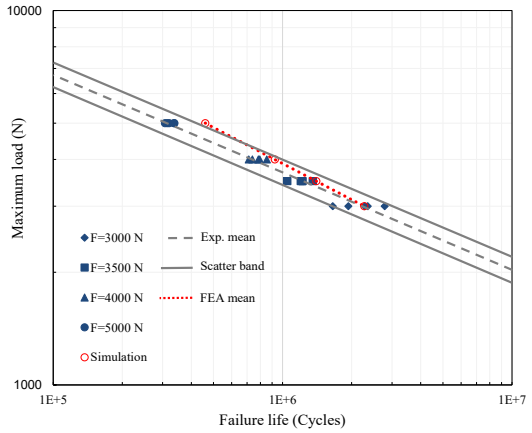

Figure 8. Fatigue performance of free-defect RSW joint: experimental testing vs. FE modeling outcomes

fatigue predictions and the corresponding experimental axial fatigue test results for defect-free three-sheet spot-welded joints. For a quantitative assessment of the model's accuracy, a comparative analysis of the experimental and simulated fatigue lives at various load levels is presented in Table 6. The results presented in the experimental life column are the average results for different replicates.

The results demonstrate a strong correlation between the simulation and experimental data. The error percentage across all tested load levels ranges from a minimum of 3.2 % to a maximum of 16.81 %, with an average error of 10.02 %. This level of deviation is considered highly acceptable for complex thermo-mechanical-fatigue simulations, given the inherent uncertainties in material properties, experimental variability (as evidenced by the scatter in the test data), and the necessary simplifications in the finite element model.

The highest errors are typically observed at higher load levels (low-cycle fatigue regime), where local plasticity and microstructural variations have a more pronounced effect that is challenging to model perfectly. Conversely, the model exhibits excellent agreement in the high-cycle fatigue regime, which is the primary focus of this study. This validation provides high confidence in the subsequent simulation results for defective joints presented in the following sections.

5. 2. Results of RSW Joints with Edge Defect

Figure 9(a) presents the force-displacement curves obtained from finite element tensile test simulations for RSW joints containing edge defects of varying severities. The relationship between edge defect severity and the maximum force—representing the joint's tensile capacity—is further illustrated in Figure 9(b). The simulation results indicate a decreasing trend in tensile strength as the edge defect becomes more pronounced. This reduction is primarily attributed to incomplete formation of the weld nugget at the defect site. For instance, a joint exhibiting an edge defect severity of 0.2 demonstrates a tensile strength of 8512.98 N, compared to 8997.4 N for the defect-free counterpart—corresponding to a 5.4% reduction in load-bearing capacity.

Furthermore, Table 7 summarizes the fatigue analysis results for joints with varying levels of edge defect

TABLE 6. Comparative analysis of experimental and simulated fatigue life for defect-free joints

Applied load (N)	Experimental life (Cycle)	Simulated life (Cycle)	Error (%)
3000	2200160	2270636	3.2
3500	1207809	1312658	8.68
4000	776387	864592	11.36
5000	323012	377319	16.81

severity, providing additional insight into the mechanical degradation associated with such imperfections.

The analysis shows that an increase in edge defect severity leads to a noticeable decline in fatigue life under identical cyclic loading conditions. For instance, when the defect severity reaches 0.2, the number of cycles to failure is reduced by approximately 13.72% compared to that of a defect-free joint.

5. 3. Results of RSW Joints with Intersection Defect

Figure 10(a) presents force-displacement diagrams of three-sheet spot-welded joints with intersection defects at different intensities as a result of the tensile analysis. In addition, tensile strength variations related to the severity of the intersection defect are displayed in Figure 10(b).

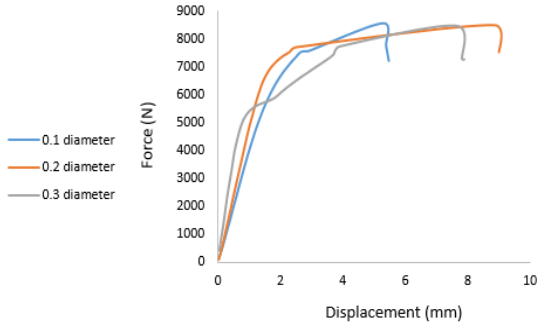

(a)

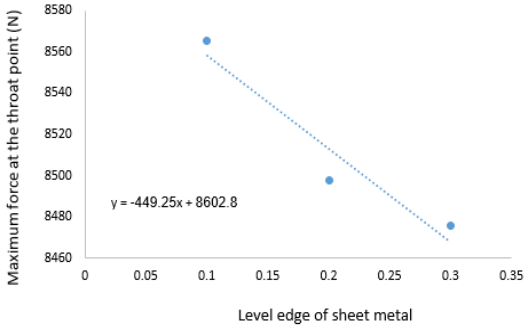

(b)

Figure 9. Static simulation results of RSW joints with edge defects at different intensities: (a) Force-displacement diagrams and (b) Tensile strength in terms of severity of the edge defect

TABLE 7. Fatigue analysis outputs for RSW joint with edge defect: cycle to failure

Edge defect severity	Max. applied load: 5000 N	Max. applied load: 4000 N
0.1	25444	49851
0.2	14501	45363
0.3	10562	34511

The findings demonstrate that the tensile strength of the spot-welded joint declines progressively as the severity of the intersection defect increases. Notably, when the defect reaches 0.8 times the nugget diameter, a substantial reduction in static strength is observed. Next, fatigue performance corresponding to various intersection defect severities is summarized in Table 8.

The results show that the fatigue life reduction in intersection defects is much greater than in edge defects. One of the most important reasons for this is the smaller weld core diameter in the joint with intersection defects compared to edge defects. For instance, when there is an intersection defect severity of 0.6, the fatigue life of the

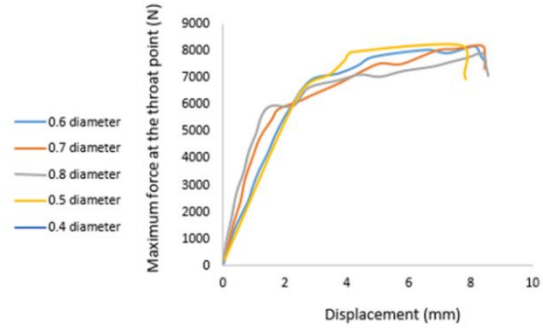

(a)

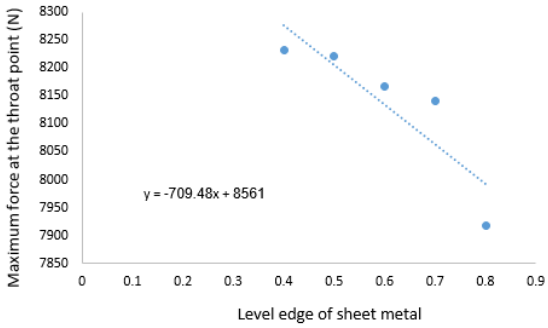

(b)

Figure 10. Static simulation results of three-sheet spot-welded joints with intersection defects at different intensities: (a) Force-displacement diagrams and (b) Tensile strength variations regarding the severity of intersection defect.

TABLE 8. Fatigue analysis outputs for RSW joint with intersection defect: cycle to failure

Edge defect severity	Max. applied load: 5000 N	Max. applied load: 4000 N
0.4	6226	28444
0.5	4877	22155
0.6	4761	21987
0.7	4321	21549
0.8	4217	20981

connection is reduced by about 54% compared to a healthy connection.

6. CONCLUSION

The main conclusions drawn from this research are outlined below:
- FE simulations of tensile and fatigue analysis for edge defect in a three-sheet spot-welded joint showed that the joint strength decreases by 5.4 % and 13.72 %, respectively, for edge defect with a specification of 0.2 to the nugget diameter. These values were reported in comparison to the strength of a defect-free weld joint under various loadings.
- FE analyses demonstrated that when the intersection defect extended beyond 60% of the nugget diameter, the corresponding tensile and fatigue strengths declined by 9.6 % and 54 %, respectively.
- For both edge and intersection defects, tensile and fatigue diagrams were extracted and reported in terms of defect severity through finite element simulation.
- The results show that RSW joint with the desired apparent defects under cyclic loading conditions may have a strength reduction of more than 50 %, therefore, following the initial hypothesis in this study, it is proposed to change the name of this type of defect to apparent-quasi-strength defects.

7. ACKNOWLEDGMENTS

This paper has been supported by the RUDN University Strategic Academic Leadership Program. Project No. 011600-0-000 " Development of technologies for creating intelligent systems and automation of production processes".

8. REFERENCES

1. Oikawa H, Murayama G, Hiwatashi S, Matsuyama K. Resistance spot weldability of high strength steel sheets for automobiles and the quality assurance of joints. Welding in the World. 2007;51(3):7-18. https://doi.org/10.1007/BF03266555
2. Tsai C, Papritan J, Dickinson D, Jammal O. Modeling of resistance spot weld nugget growth. Welding Journal(USA). 1992;71(2):47.
3. Amiri N, Farrahi G, Kashyzadeh KR, Chizari M. Applications of ultrasonic testing and machine learning methods to predict the static & fatigue behavior of spot-welded joints. Journal of Manufacturing Processes. 2020;52:26-34. https://doi.org/10.1016/j.jmapro.2020.01.047
4. Patil SA, Baratzadeh F, Lankarani H. Modeling of the weld strength in spot weld using regression analysis of the stress parameters based on the simulation study. Journal of Materials Science Research. 2017;6:51-62.
5. Martín Ó, Pereda M, Santos JI, Galán JM. Assessment of resistance spot welding quality based on ultrasonic testing and tree-based techniques. Journal of Materials Processing Technology. 2014;214(11):2478-87. https://doi.org/10.1016/j.jmatprotec.2014.05.021
6. Farrahi G, Ahmadi A, Kasyzadeh KR. Simulation of vehicle body spot weld failures due to fatigue by considering road roughness and vehicle velocity. Simulation Modelling Practice and Theory. 2020;105:102168. https://doi.org/10.1016/j.simpat.2020.102168
7. Liu W, Hu J, Qi J. Resistance Spot Welding Defect Detection Based on Visual Inspection: Improved Faster R-CNN Model. Machines. 2025;13(1):33. https://doi.org/10.3390/machines13010033
8. Summerville C, Adams D, Compston P, Doolan M. Nugget diameter in resistance spot welding: a comparison between a dynamic resistance based approach and ultrasound C-scan. Procedia Engineering. 2017;183:257-63. https://doi.org/10.1016/j.proeng.2017.04.033
9. Mirzaei F, Ghorbani H, Kolahan F. Numerical modeling and optimization of joint strength in resistance spot welding of galvanized steel sheets. The International Journal of Advanced Manufacturing Technology. 2017;92(9):3489-501. https://doi.org/10.1007/s00170-017-0407-x
10. Eshraghi M, Tschopp MA, Zaeem MA, Felicelli SD, editors. A parametric study of resistance spot welding of a dual-phase steel using finite element analysis. Proceedings of the 8th Pacific Rim International Congress on Advanced Materials and Processing; 2013: Springer.
11. Eisazadeh H, Hamedi M, Halvaee A. New parametric study of nugget size in resistance spot welding process using finite element method. Materials & Design. 2010;31(1):149-57. https://doi.org/10.1016/j.matdes.2009.06.042
12. Chuenmee N, Phothi N, Chamniprasart K, Khaengkarn S, Srisertpol J. Machine learning for predicting resistance spot weld quality in automotive manufacturing. Results in Engineering. 2025;25:103570. https://doi.org/10.1016/j.rineng.2024.103570
13. Moshayedi H, Sattari-Far I. Numerical and experimental study of nugget size growth in resistance spot welding of austenitic stainless steels. Journal of Materials Processing Technology. 2012;212(2):347-54. https://doi.org/10.1016/j.jmatprotec.2011.09.004
14. Farrahi G, Ahmadi A, Kashyzadeh KR, Azadi S, Jahani K. A comparative study on the fatigue life of the vehicle body spot welds using different numerical techniques: Inertia relief and Modal dynamic analyses. Fracture and Structural Integrity. 2020;14(52):67-81. https://doi.org/10.3221/IGF-ESIS.52.06
15. Pan N, Sheppard S. Spot welds fatigue life prediction with cyclic strain range. International Journal of Fatigue. 2002;24(5):519-28. https://doi.org/10.1016/S0142-1123(01)00157-8
16. Kashyzadeh KR, Ghorbani S. High-cycle fatigue behavior and chemical composition empirical relationship of low carbon three-sheet spot-welded joint: An application in automotive industry. Journal of Design Against Fatigue. 2023;1(2):1-8.
17. Deshmukh DD, Kharche Y. Influence of processing conditions on the tensile strength and failure pattern of resistance spot welded SS 316L sheet joint. International Journal on Interactive Design and Manufacturing (IJIDeM). 2025;19(1):559-71. https://doi.org/10.1007/s12008-023-01465-8
18. Nodeh IR, Serajzadeh S, Kokabi AH. Simulation of welding residual stresses in resistance spot welding, FE modeling and X-ray verification. Journal of materials processing technology. 2008;205(1-3):60-9. https://doi.org/10.1016/j.jmatprotec.2007.11.104
19. Maleki E, Unal O, Kashyzadeh KR. Surface layer nanocrystallization of carbon steels subjected to severe shot peening: Analysis and optimization. Materials Characterization. 2019;157:109877. https://doi.org/10.1016/j.matchar.2019.109877

20. Maleki E, Unal O, Kashyzadeh KR. Fatigue behavior prediction and analysis of shot peened mild carbon steels. International Journal of Fatigue. 2018;116:48-67. https://doi.org/10.1016/j.ijfatigue.2018.06.004
21. Pal TK, Bhowmick K. Resistance spot welding characteristics and high cycle fatigue behavior of DP 780 steel sheet. Journal of Materials Engineering and Performance. 2012;21(2):280-5. https://doi.org/10.1007/s11665-011-9850-2
22. Xiao L, Liu L, Chen D, Esmaeili S, Zhou Y. Resistance spot weld fatigue behavior and dislocation substructures in two different heats of AZ31 magnesium alloy. Materials Science and Engineering: A. 2011;529:81-7. https://doi.org/10.1016/j.msea.2011.08.064
23. Ordoñez J, Ambriz R, García C, Plascencia G, Jaramillo D. Overloading effect on the fatigue strength in resistance spot welding joints of a DP980 steel. International Journal of Fatigue. 2019;121:163-71. https://doi.org/10.1016/j.ijfatigue.2018.12.026
24. Hassanifard S, Zehsaz M, Esmaeili F. Spot weld arrangement effects on the fatigue behavior of multi-spot welded joints. Journal of mechanical science and technology. 2011;25(3):647-53. https://doi.org/10.1007/s12206-011-0112-x
25. Esmaeili F, Rahmani A, Barzegar S, Afkar A. Prediction of fatigue life for multi-spot welded joints with different arrangements using different multiaxial fatigue criteria. Materials & Design. 2015;72:21-30. https://doi.org/10.1016/j.matdes.2015.02.008
26. Vural M, Akkuş A, Eryürek B. Effect of welding nugget diameter on the fatigue strength of the resistance spot welded joints of different steel sheets. Journal of Materials Processing Technology. 2006;176(1-3):127-32. https://doi.org/10.1016/j.jmatprotec.2006.02.026
27. Reza Kashyzadeh K, Farrahi G, Ahmadi A, Minaei M, Ostad Rahimi M, Barforoushan S. Fatigue life analysis in the residual stress field due to resistance spot welding process considering different sheet thicknesses and dissimilar electrode geometries. Proceedings of the Institution of Mechanical Engineers, Part L: Journal of Materials: Design and Applications. 2023;237(1):33-51. https://doi.org/10.1177/14644207221101069
28. Farrahi G, Kashyzadeh KR, Minaei M, Sharifpour A, Riazi S. Analysis of resistance spot welding process parameters effect on the weld quality of three-steel sheets used in automotive industry: Experimental and finite element simulation. International Journal of Engineering Transactions A: Basics. 2020;33(1):148-57. https://doi.org/10.5829/ije.2020.33.01a.17
29. Ganjabi MA, Farrahi G, Reza Kashyzadeh K, Amiri N. Effects of various strength defects of spot weld on the connection strength under both static and cyclic loading conditions: empirical and numerical investigation. The International Journal of Advanced Manufacturing Technology. 2023;127(11):5665-78. https://doi.org/10.1007/s00170-023-11923-y
30. ISO14324 RSWDT. of Welds-Method for the Fatigue Testing of Spot Welded Joints. The International Organization for Standardization. 2003. https://www.iso.org/standard/24088.html
31. Hong JK. The development of a simplified spot weld model for Battelle structural stress calculation. SAE International Journal of Materials and Manufacturing. 2011;4(1):602-12. https://doi.org/10.4271/2011-01-0479
32. Dong P, Prager M, Osage D. The design master SN curve in ASME Div 2 rewrite and its validations. Welding in the World. 2007;51(5):53-63. https://doi.org/10.1007/BF03266573

Persian Abstract

چکیده

تکنیک جوشکاری مقاومتی نقطه‌ای روشی رایج برای اتصال ورق‌های فلزی نازک در صنایع مرتبط با حمل و نقل مانند خودرو و هوافضا است. مزیت کلیدی این اتصال در کارآیی آن و عدم نیاز به مواد اضافی است که به کاهش وزن سازه کمک می‌کند. در این مطالعه، تاثیر عیوب قابل مشاهده (یعنی لبه و تقاطع) بر رفتار مکانیکی اتصالات جوش داده شده سه ورقی تحت بارهای استاتیکی و خستگی مورد تجزیه و تحلیل قرار گرفته است. برای این منظور، ترکیبی از تست‌های آزمایشگاهی و مدلسازی اجزای محدود مورد استفاده قرار گرفت. رویکرد اجزای محدود با استفاده از داده‌های تجربی خستگی محوری (منحنی‌های تنش–عمر در ناحیه پرچرخه) اعتبارسنجی شد. بر خلاف تحقیقات قبلی، این تحقیق برای اولین بار چنین نقص‌های سطحی را در چارچوب مدل اجزای محدود گنجانده است. نتایج شبیه‌سازی نشان داد که یک عیب لبه با شدت ۰.۲ میلی‌متری منجر به کاهش استحکام کششی و خستگی به ترتیب ۵.٤ و ۱۳.۷۲ درصد می‌شود، در حالی که یک عیب تقاطع با شدت ۰.٦ میلی‌متری باعث کاهش ۹.٦ و ٥٤ درصدی به ترتیب در استحکام کششی و خستگی می‌شود. این یافته‌ها حساسیت بیشتر استحکام خستگی به چنین نقص‌هایی را در مقایسه با استحکام کششی برجسته می‌کند.